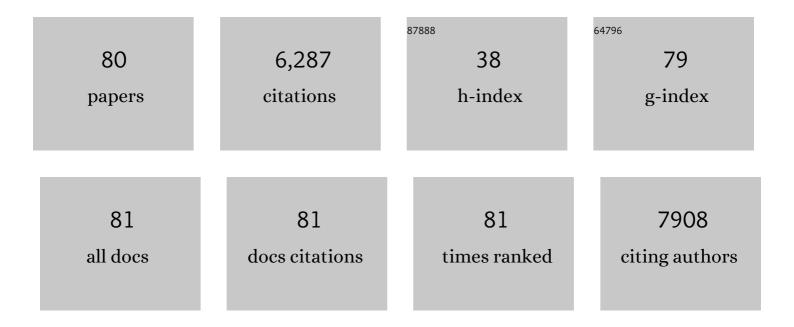
Guohui Tian

List of Publications by Year in descending order

Source: https://exaly.com/author-pdf/2167089/publications.pdf Version: 2024-02-01



#	Article	IF	CITATIONS
1	Boosted charge transfer and photocatalytic CO2 reduction over sulfur-doped C3N4 porous nanosheets with embedded SnS2-SnO2 nanojunctions. Science China Materials, 2022, 65, 400-412.	6.3	21
2	Fabrication of size-controlled hierarchical ZnS@ZnIn2S4 heterostructured cages for enhanced gas-phase CO2 photoreduction. Journal of Colloid and Interface Science, 2022, 605, 253-262.	9.4	47
3	Efficient charge transfer in cadmium sulfide quantum dot-decorated hierarchical zinc sulfide-coated tin disulfide cages for carbon dioxide photoreduction. Journal of Colloid and Interface Science, 2022, 615, 606-616.	9.4	5
4	Hierarchical CuS@ZnIn ₂ S ₄ Hollow Double-Shelled p–n Heterojunction Octahedra Decorated with Fullerene C ₆₀ for Remarkable Selectivity and Activity of CO ₂ Photoreduction into CH ₄ . ACS Applied Materials & Interfaces, 2022, 14, 7888-7899.	8.0	34
5	Efficient charge transfer and CO2 photoreduction of hierarchical CeO2@SnS2 heterostructured hollow spheres with spatially separated active sites. Applied Surface Science, 2022, 592, 153192.	6.1	13
6	Sandwich-Structured Hybrid of NiCo Nanoparticles-Embedded Carbon Nanotubes Grafted on C ₃ N ₄ Nanosheets for Efficient Photodehydrogenative Coupling Reactions. ACS Applied Materials & Interfaces, 2022, 14, 24425-24434.	8.0	14
7	Hierarchical CuCo ₂ S ₄ Nanoflake Arrays Grown on Carbon Cloth: A Remarkable Bifunctional Electrocatalyst for Overall Water Splitting. ChemElectroChem, 2021, 8, 1134-1140.	3.4	19
8	Cu2O decorated α-Fe2O3/SnS2 core/shell heterostructured nanoarray photoanodes for water splitting. Solar Energy, 2021, 220, 843-851.	6.1	12
9	Hierarchical Co _{0.85} Se dSe/MoSe ₂ /CdSe Sandwichâ€Like Heterostructured Cages for Efficient Photocatalytic CO ₂ Reduction. Small, 2021, 17, e2100412.	10.0	29
10	Improved charge separation and carbon dioxide photoreduction performance of surface oxygen vacancy-enriched zinc ferrite@titanium dioxide hollow nanospheres with spatially separated cocatalysts. Journal of Colloid and Interface Science, 2021, 599, 1-11.	9.4	15
11	Sulfur doped In2O3-CeO2 hollow hexagonal prisms with carbon coating for efficient photocatalytic CO2 reduction. Chemical Engineering Journal, 2021, 421, 129968.	12.7	52
12	Surface oxygen vacancy defect-promoted electron-hole separation for porous defective ZnO hexagonal plates and enhanced solar-driven photocatalytic performance. Chemical Engineering Journal, 2020, 379, 122295.	12.7	170
13	In situ intercalation and exploitation of Co3O4 nanoparticles grown on carbon nitride nanosheets for highly efficient degradation of methylene blue. Dalton Transactions, 2020, 49, 14665-14672.	3.3	12
14	Efficient Separation of Photogenerated Charges in Sandwiched Bi ₂ S ₃ â`BiOCl Nanoarrays/BiVO ₄ Nanosheets Composites for Enhanced Photocatalytic Activity. ChemCatChem, 2020, 12, 3223-3229.	3.7	5
15	Hierarchical ZnO nanorod/ZnFe2O4 nanosheet core/shell nanoarray decorated with PbS quantum dots for efficient photoelectrochemical water splitting. Journal of Alloys and Compounds, 2020, 828, 154449.	5.5	28
16	Hierarchical NiS decorated CuO@ZnFe2O4 nanoarrays as advanced photocathodes for hydrogen evolution reaction. International Journal of Hydrogen Energy, 2020, 45, 6174-6183.	7.1	19
17	Achieving cadmium selenide-decorated zinc ferrite@titanium dioxide hollow core/shell nanospheres with improved light trapping and charge generation for photocatalytic hydrogen generation. Journal of Colloid and Interface Science, 2020, 575, 158-167.	9.4	16
18	Ultrathin-layered MoS2 hollow nanospheres decorating Ni3S2 nanowires as high effective self-supporting electrode for hydrogen evolution reaction. International Journal of Hydrogen Energy, 2020, 45, 13149-13162.	7.1	31

#	Article	IF	CITATIONS
19	Controlled synthesis and exceptional photoelectrocatalytic properties of Bi2S3/MoS2/Bi2MoO6 ternary hetero-structured porous film. Journal of Colloid and Interface Science, 2019, 555, 214-223.	9.4	26
20	Surface-oxygen vacancy defect-promoted electron-hole separation of defective tungsten trioxide ultrathin nanosheets and their enhanced solar-driven photocatalytic performance. Journal of Colloid and Interface Science, 2019, 557, 18-27.	9.4	14
21	WO3/BiVO4/BiOCl porous nanosheet composites from a biomass template for photocatalytic organic pollutant degradation. Journal of Alloys and Compounds, 2019, 802, 76-85.	5.5	39
22	Homojunction and defect synergy-mediated electron–hole separation for solar-driven mesoporous rutile/anatase TiO ₂ microsphere photocatalysts. RSC Advances, 2019, 9, 7870-7877.	3.6	18
23	Hierarchical Cu7S4-Cu9S8 heterostructure hollow cubes for photothermal aerobic oxidation of amines. Chemical Engineering Journal, 2019, 363, 247-258.	12.7	45
24	Hierarchical SnS ₂ /CuInS ₂ Nanosheet Heterostructure Films Decorated with C ₆₀ for Remarkable Photoelectrochemical Water Splitting. ACS Applied Materials & Interfaces, 2019, 11, 9093-9101.	8.0	68
25	Nickel–Cobalt Diselenide Nanosheets Supported on Copper Nanowire Arrays for Synergistic Electrocatalytic Oxygen Evolution. Advanced Materials Interfaces, 2019, 6, 1802052.	3.7	22
26	Surface Plasmon Resonanceâ€Enhanced Visibleâ€NIRâ€Driven Photocatalytic and Photothermal Catalytic Performance by Ag/Mesoporous Black TiO ₂ Nanotube Heterojunctions. Chemistry - an Asian Journal, 2019, 14, 177-186.	3.3	39
27	Tuning in BiVO4/Bi4V2O10 porous heterophase nanospheres for synergistic photocatalytic degradation of organic pollutants. Applied Surface Science, 2019, 470, 631-638.	6.1	20
28	Molecule Self-Assembly Synthesis of Porous Few-Layer Carbon Nitride for Highly Efficient Photoredox Catalysis. Journal of the American Chemical Society, 2019, 141, 2508-2515.	13.7	685
29	Enhanced charge transfer and separation of hierarchical hydrogenated TiO ₂ nanothorns/carbon nanofibers composites decorated by NiS quantum dots for remarkable photocatalytic H ₂ production activity. Nanoscale, 2018, 10, 4041-4050.	5.6	39
30	Highly dispersed of Ni0.85Se nanoparticles on nitrogen-doped graphene oxide as efficient and durable electrocatalyst for hydrogen evolution reaction. Electrochimica Acta, 2018, 262, 107-114.	5.2	39
31	Exceptional visible-light photoelectrocatalytic activity of In2O3/In2S3/CdS ternary stereoscopic porous heterostructure film for the degradation of persistent 4-fluoro-3-methylphenol. Applied Catalysis B: Environmental, 2018, 225, 477-486.	20.2	66
32	Hydrogenated Cu ₂ OAu@CeO ₂ Z-scheme catalyst for photocatalytic oxidation of amines to imines. Catalysis Science and Technology, 2018, 8, 5535-5543.	4.1	23
33	NiSeâ€Ni _{0.85} Se Heterostructure Nanoflake Arrays on Carbon Paper as Efficient Electrocatalysts for Overall Water Splitting. Small, 2018, 14, e1800763.	10.0	185
34	Surface defect-mediated efficient electron-hole separation in hierarchical flower-like bismuth molybdate hollow spheres for enhanced visible-light-driven photocatalytic performance. Journal of Colloid and Interface Science, 2018, 531, 664-671.	9.4	25
35	Assembly of TiO2 ultrathin nanosheets with surface lattice distortion for solar-light-driven photocatalytic hydrogen evolution. Applied Catalysis B: Environmental, 2018, 239, 317-323.	20.2	77
36	Self-floating amphiphilic black TiO2 foams with 3D macro-mesoporous architectures as efficient solar-driven photocatalysts. Applied Catalysis B: Environmental, 2017, 206, 336-343.	20.2	102

#	Article	IF	CITATIONS
37	Cubic quantum dot/hexagonal microsphere Znln ₂ S ₄ heterophase junctions for exceptional visible-light-driven photocatalytic H ₂ evolution. Journal of Materials Chemistry A, 2017, 5, 8451-8460.	10.3	176
38	Self‣upported NiS Nanoparticle oupled Ni ₂ P Nanoflake Array Architecture: An Advanced Catalyst for Electrochemical Hydrogen Evolution. ChemElectroChem, 2017, 4, 1341-1348.	3.4	17
39	Hydrogenated TiO2/SrTiO3 porous microspheres with tunable band structure for solar-light photocatalytic H2 and O2 evolution. Science China Materials, 2016, 59, 1003-1016.	6.3	32
40	In situ formation of a ZnO/ZnSe nanonail array as a photoelectrode for enhanced photoelectrochemical water oxidation performance. Nanoscale, 2016, 8, 9366-9375.	5.6	52
41	Facile strategy for controllable synthesis of stable mesoporous black TiO ₂ hollow spheres with efficient solar-driven photocatalytic hydrogen evolution. Journal of Materials Chemistry A, 2016, 4, 7495-7502.	10.3	198
42	Large-scale synthesis of stable mesoporous black TiO ₂ nanosheets for efficient solar-driven photocatalytic hydrogen evolution via an earth-abundant low-cost biotemplate. RSC Advances, 2016, 6, 50506-50512.	3.6	29
43	Black N/Hâ€īiO ₂ Nanoplates with a Flowerâ€Like Hierarchical Architecture for Photocatalytic Hydrogen Evolution. ChemSusChem, 2016, 9, 2841-2848.	6.8	73
44	Facile Strategy to Fabricate Uniform Black TiO ₂ Nanothorns/Graphene/Black TiO ₂ Nanothorns Sandwichlike Nanosheets for Excellent Solarâ€Driven Photocatalytic Performance. ChemCatChem, 2016, 8, 3240-3246.	3.7	21
45	Hydrogenated CeO _{2â^'x} S _x mesoporous hollow spheres for enhanced solar driven water oxidation. Chemical Communications, 2016, 52, 2521-2524.	4.1	21
46	Carbothermal synthesis of ordered mesoporous carbon-supported nano zero-valent iron with enhanced stability and activity for hexavalent chromium reduction. Journal of Hazardous Materials, 2016, 309, 249-258.	12.4	131
47	Hierarchical Ag/Ag ₂ S/CuS Ternary Heterostructure Composite as an Efficient Visibleâ€Light Photocatalyst. ChemCatChem, 2015, 7, 1684-1690.	3.7	23
48	Single-crystalline Bi ₁₉ Br ₃ S ₂₇ nanorods with an efficiently improved photocatalytic activity. CrystEngComm, 2015, 17, 6120-6126.	2.6	17
49	One-step synthesis of a hierarchical Bi ₂ S ₃ nanoflowerIn ₂ S ₃ nanosheet composite with efficient visible-light photocatalytic activity. CrystEngComm, 2015, 17, 8720-8727.	2.6	38
50	Hierarchical FeTiO ₃ –TiO ₂ hollow spheres for efficient simulated sunlight-driven water oxidation. Nanoscale, 2015, 7, 15924-15934.	5.6	50
51	Hierarchical Nâ€Doped TiO ₂ Microspheres with Exposed (001) Facets for Enhanced Visible Light Catalysis. European Journal of Inorganic Chemistry, 2014, 2014, 2146-2152.	2.0	29
52	Enhanced Photocatalytic Hydrogen Evolution over Hierarchical Composites of ZnIn ₂ S ₄ Nanosheets Grown on MoS ₂ Slices. Chemistry - an Asian Journal, 2014, 9, 1291-1297.	3.3	57
53	Hierarchical composites of TiO2 nanowire arrays on reduced graphene oxide nanosheets with enhanced photocatalytic hydrogen evolution performance. Journal of Materials Chemistry A, 2014, 2, 4366-4374.	10.3	112
54	In situ growth of Bi ₂ MoO ₆ on reduced graphene oxide nanosheets for improved visible-light photocatalytic activity. CrystEngComm, 2014, 16, 842-849.	2.6	80

#	Article	IF	CITATIONS
55	Hierarchical Core–Shell Carbon Nanofiber@ZnIn ₂ S ₄ Composites for Enhanced Hydrogen Evolution Performance. ACS Applied Materials & Interfaces, 2014, 6, 13841-13849.	8.0	179
56	Fabrication of noncovalently functionalized brick-like β-cyclodextrins/graphene composite dispersions with favorable stability. RSC Advances, 2014, 4, 2813-2819.	3.6	14
57	Growth rate controlled synthesis of hierarchical Bi2S3/In2S3 core/shell microspheres with enhanced photocatalytic activity. Scientific Reports, 2014, 4, 4027.	3.3	108
58	Composites of small Ag clusters confined in the channels of well-ordered mesoporous anatase TiO2 and their excellent solar-light-driven photocatalytic performance. Nano Research, 2014, 7, 731-742.	10.4	102
59	A Floating Porous Crystalline TiO ₂ Ceramic with Enhanced Photocatalytic Performance for Wastewater Decontamination. European Journal of Inorganic Chemistry, 2013, 2013, 2411-2417.	2.0	59
60	Controlled synthesis of mesoporous anatase TiO2 microspheres as a scattering layer to enhance the photoelectrical conversion efficiency. Journal of Materials Chemistry A, 2013, 1, 9853.	10.3	70
61	Single-step pyrolytic preparation of Mo2C/graphitic carbon nanocomposite as catalyst carrier for the direct liquid-feed fuel cells. RSC Advances, 2013, 3, 4771.	3.6	27
62	Facile synthesis and shape control of Fe3O4 nanocrystals with good dispersion and stabilization. CrystEngComm, 2013, 15, 3366.	2.6	19
63	Hierarchical flake-like Bi2MoO6/TiO2 bilayer films for visible-light-induced self-cleaning applications. Journal of Materials Chemistry A, 2013, 1, 6961.	10.3	102
64	Hierarchical Composite of Ag/AgBr Nanoparticles Supported on Bi ₂ MoO ₆ Hollow Spheres for Enhanced Visible‣ight Photocatalytic Performance. ChemPlusChem, 2013, 78, 117-123.	2.8	58
65	Hierarchical CuS hollow nanospheres and their structure-enhanced visible light photocatalytic properties. CrystEngComm, 2013, 15, 5144.	2.6	106
66	Confinement Effect on Ag Clusters in the Channels of Wellâ€Ordered Mesoporous TiO ₂ and their Enhanced Photocatalytic Performance. ChemCatChem, 2013, 5, 1354-1358.	3.7	13
67	Facile synthesis of sheet-like ZnO assembly composed of small ZnO particles for highly efficient photocatalysis. Journal of Materials Chemistry A, 2013, 1, 5700.	10.3	170
68	A facile and green synthesis route towards two-dimensional TiO2@Ag heterojunction structure with enhanced visible light photocatalytic activity. CrystEngComm, 2013, 15, 5821.	2.6	25
69	Controlled synthesis of thorny anatase TiO ₂ tubes for construction of Ag–AgBr/TiO ₂ composites as highly efficient simulated solar-light photocatalyst. Journal of Materials Chemistry, 2012, 22, 2081-2088.	6.7	84
70	Room temperature solution synthesis of hierarchical bow-like Cu2O with high visible light driven photocatalytic activity. RSC Advances, 2012, 2, 2875.	3.6	38
71	Facile preparation of porous NiTiO3 nanorods with enhanced visible-light-driven photocatalytic performance. Journal of Materials Chemistry, 2012, 22, 16471.	6.7	176
72	Fabrication of Rice‣ike Porous Anatase TiO ₂ with High Thermal Stability and Enhanced Photocatalytic Performance. ChemCatChem, 2012, 4, 844-850.	3.7	17

#	Article	IF	CITATIONS
73	Facile solvothermal synthesis of hierarchical flower-like Bi ₂ MoO ₆ hollow spheres as high performance visible-light driven photocatalysts. Journal of Materials Chemistry, 2011, 21, 887-892.	6.7	427
74	3D hierarchical flower-like TiO2 nanostructure: morphology control and its photocatalytic property. CrystEngComm, 2011, 13, 2994.	2.6	237
75	Wellâ€Ordered Largeâ€Pore Mesoporous Anatase TiO ₂ with Remarkably High Thermal Stability and Improved Crystallinity: Preparation, Characterization, and Photocatalytic Performance. Advanced Functional Materials, 2011, 21, 1922-1930.	14.9	431
76	Solvothermal Synthesis, Characterization, and Formation Mechanism of a Single‣ayer Anatase TiO ₂ Nanosheet with a Porous Structure. European Journal of Inorganic Chemistry, 2011, 2011, 754-760.	2.0	22
77	Dyeâ€Sensitised Solar Cells Based on Largeâ€Pore Mesoporous TiO ₂ with Controllable Pore Diameters. European Journal of Inorganic Chemistry, 2011, 2011, 4730-4737.	2.0	12
78	Synthesis and photocatalytic activity of stable nanocrystalline TiO2 with high crystallinity and large surface area. Journal of Hazardous Materials, 2009, 161, 1122-1130.	12.4	172
79	Enhanced photocatalytic activity of S-doped TiO2–ZrO2 nanoparticles under visible-light irradiation. Journal of Hazardous Materials, 2009, 166, 939-944.	12.4	101
80	Preparation and Characterization of Stable Biphase TiO ₂ Photocatalyst with High Crystallinity, Large Surface Area, and Enhanced Photoactivity. Journal of Physical Chemistry C, 2008, 112, 3083-3089.	3.1	288

6